NASA

Technical Memorandum 86092

THERMAL DETECTORS AS X-RAY SPECTROMETERS

S.H. Moseley, J.C. Mather, and D. McCammon

APRIL 1984

National Aeronautics and
Space Administration

Goddard Space Flight Center
Greenbelt, Maryland 20771

Thermal Detectors as X-Ray Spectrometers

S. H. Moseley

J. C. Mather

Goddard Space Flight Center

Greenbelt, MD 20771

D. McCammon

Department of Physics

University of Wisconsin

Madison, WI 53706

Abstract

We show that sensitive thermal detectors should be useful for measuring very small energy pulses, such as those produced by the absorption of x-ray photons. The measurement uncertainty can be very small, making the technique promising for high resolution nondispersive x-ray spectroscopy.

We derive the limits to the energy resolution of such thermal detectors. We use these to find the resolution to be expected for a detector suitable for x-ray spectroscopy in the 100-10,000 eV range. If there is no noise in the thermalization of the x-ray, resolution better than 1 eV full width at half maximum (FWHM) is possible for detectors operating at 0.1 K.

Energy loss in the conversion of the photon energy to heat is a potential problem. Statistical fluctuations of lost energy would reduce the energy resolution of the detector. The loss mechanisms may include emission of photons or electrons, or the trapping of energy in long-lived metastable states. Fluctuations in the phonon spectrum could also limit the resolution if phonon relaxation times are very long. We give conceptual solutions for each of these possible problems.

I. Introduction

An ultimate goal for any spectrometer is to offer high resolving power and throughput simultaneously over a wide energy range. Silicon solid state diode detectors used as x-ray spectrometers have good efficiency but their resolution is only 100-200 eV. Wavelength dispersive spectrometers offer resolution $\leq$ 10 eV, but have low throughputs. A thermal detector operating at cryogenic temperatures can offer the high efficiency of the solid state detector and resolution comparable to that of dispersive spectrometers.

Bolometers have been used for many years as infrared detectors (Low, 1961). Recent work[1,2,3] shows that at temperatures as low as 0.32 K, the dominant noise in properly constructed devices is due to the thermodynamic fluctuations in the device itself.

The energy sensitivity of a thermal detector scales as $T\sqrt{C}$ where T is the operating temperature and C the detector heat capacity. Practical designs for detectors can be made using the substantial body of low temperature data existing in the literature. An operating temperature of 0.1 K has been chosen as the design temperature because it permits the desired resolution, and it can easily be achieved with an adiabatic demagnetization refrigerator operating with a 2 K heat sink. Also, experimental data show that the heat capacities of many of our candidate materials decline quite slowly or actually increase below 0.1 K.

We will demonstrate that the noise in the front end amplifier junction field effect transistor (JFET) and load resistor need not seriously affect the resolution.

The performance of a bolometer as an x-ray spectrometer depends on the noiseless conversion of the x-ray to heat. If some fraction of the energy is lost, that fraction need not be exactly constant from photon to photon. This will degrade the resolution of the spectrometer. We will discuss potential loss mechanisms and techniques for combatting them.

II. Theory of Operation

A typical bolometer detector has three parts: an energy absorber, a semiconducting thermometer, and a support structure to carry away the applied heat and establish electrical contact to the thermometer. A design for such a detector is given in Figure 1 and discussed in Section IV. The detector temperature is measured by applying a DC bias voltage to the series combination of the thermometer and a load resistor. Small variations in the thermistor voltage are measured using a low noise amplifier, whose first stage is usually a JFET source follower mounted near the detector but operating at about 80 K.

The basic theory of these detectors has been summarized.[4,5] A more complete theory has been given by Mather,[6] and optimization for their use as power detectors has been carried out.[7]

Resolution

An order of magnitude estimate of the possible energy resolution is given by the thermodynamic energy fluctuations in the detector. From the derivatives of the partition function for a system, one finds easily that

$$\langle \Delta U^2 \rangle = k_B T^2 C, \tag{1}$$

regardless of the details of the system. Here, ΔU is the spontaneous energy fluctuation of the detector, T its temperature, and C its heat capacity, and k_B is Boltzmann's constant. One can understand this in a handwaving way by saying that the effective number of phonon modes in the detector is $N = C/k_B$, the typical phonon mode has quantum occupation number 1, rms fluctuation of 1 phonon, and mean energy of kT. Then the mean square energy fluctuation is $(k_B T)^2 N = k_B T^2 C$. We show below that this expression differs from the resolution achievable in practice only by a numerical factor of ~ 2.

In addition to these thermodynamic fluctuations, or phonon noise, a more complete derivation of the energy resolution must consider Johnson noise in the thermistor, thermistor responsivity, the effects of temperature gradients in the thermal link produced by the applied bias power, and optimization of the signal shaping filters. We first discuss an approximate solution to this problem in the time domain to give a clear illustration of the nature of these effects. The exact solution is reached more readily from an analysis in the frequency domain, for which we will adapt the results of Ref. 6 and 7 to the case where the input signal is assumed to be a delta function.

We model the detector as an absorber of heat capacity C with a temperature sensor attached. The absorber is connected to the heat sink through a link of thermal conductance G. An x-ray photon of energy U incident on the absorber will be absorbed and thermalized. The temperature of the detector element rises by $\Delta T = U/C$ following the absorption of the photon. The heat flows to the heat sink through the conductive link and the detector element approaches the bath temperature exponentially with a time constant $\tau = C/G$. In a practical detector, the time constant of the output pulse is changed from the physical time constant τ by electrothermal feedback to an effective time constant τ_e.[6] Therefore in the time domain, an impulse of energy U at time $t = 0$ produces a decaying exponential pulse of voltage

$$V(t) = U \frac{S(0)}{\tau_e} e^{-t/\tau_e} , \qquad (2)$$

where S(0) is the detector responsivity at zero frequency (measured in volts/watt).

Given the output pulse shape following the absorption of an x-ray, the choice of an optimal shaping filter depends on the spectral characteristics of the detector noise. In this instructive example we will devise a solution for a white noise spectrum. For practical detectors using semiconducting thermistors, the assumption of white noise is quite good; the phonon noise and Johnson noise powers have substantial frequency dependence, but their quadrature sum does not.[6] We will divide our exponential pulse into intervals of width Δt. The estimates of U in each interval will be averaged with weights proportional to the squares of their

signal to noise ratios. Since the noise is white, each of these intervals is a statistically independent estimator of the signal. The weighted average of all these is the best estimator of the total energy. The expression for the total signal derived in this way is

$$U = \frac{2\tau_e}{S(0)} \int_0^\infty \frac{e^{-t/\tau_e}}{\tau_e} V(t)\, dt. \qquad (3)$$

In a digital signal processor, the integral can be done very easily. In the analog electronics domain, it would require passing the signal through a filter which is a time reversed (non causal) single pole RC low pass filter. This ideal filter has the same noise bandwidth as the ordinary RC filter, $B = (4\ \tau_e)^{-1}$. Since the detector has a white noise with spectral density e_n^2, the rms output of the filter in the absence of pulses is

$$\Delta U_{rms} = e_n \sqrt{B} \cdot \frac{2\tau_e}{S(0)} = NEP(0) \cdot \sqrt{\tau_e}, \qquad (4)$$

where the noise equivalent power of the detector at zero frequency is defined by $NEP(0) = e_n/S(0)$. This analysis implicitly assumes that the moment of arrival of the pulse is known. For high signal to noise pulses, this assumption is justified.

For the actual case in which the noise is not exactly white, the analysis is done more readily in the frequency domain. Here, a measurement of the noise in each frequency interval Δf is statistically independent of measurements in other intervals as long as the noise is stationary.

The result in Eq. 3 can be written in the frequency domain

$$\Delta U_{rms} = \left[\int_0^\infty \frac{4\,df}{NEP^2(f)} \right]^{-1/2}. \qquad (5)$$

For $NEP^2(f) = NEP^2(0)\ [1 + \omega^2\ \tau_e{}^2]$, the white noise voltage case, this yields the same result as above. This formula gives greatest weight to frequency regions where the NEP is small. In the frequency domain, the random temperature variation of the element gives rise to $NEP^2_{phonon} = 4k_BT^2G$ (for an element at thermal equilibrium), where G is the thermal conductance to the heat sink. It is independent of frequency, so if it were the limiting noise source over an extreme bandwidth (much larger than $1/\tau_e$), the detector resolution could be much smaller than $(k_BT^2C)^{1/2}$. This possibility is not yet of practical importance, since it requires temperature transducers much better than the semiconducting thermistor.

Optimization

We will now give detailed formulas for the NEP in the ideal bolometer, proceed to the energy resolution, and finally compute the optimum bias conditions and ultimate energy resolution of the detector. This work is based directly on Ref. 6 and parallels similar optimization calculations for infrared detectors.[7]

The square of the NEP for the ideal detector, in which amplifier noise and noise from the load resistor can be neglected, can be written

$$NEP^2 = NEP^2_{Johnson} + NEP^2_{phonon}, \tag{6}$$

where

$$NEP^2_{phonon} = N_1 = 4k_BGT^2 \int_{T_c}^{T} \left[\frac{t'k(t')}{Tk(T)}\right]^2 dt' \Big/ \int_{T_c}^{T} \left[\frac{k(t')}{k(T)}\right] dt', \tag{7}$$

$$NEP^2_{Johnson} = N_2(1+\omega^2\tau^2), \tag{8}$$

and $$N_2 = 4k_B T P \left[\frac{Z+R}{Z-R}\right]^2 \quad . \tag{9}$$

In these formulas, terms are defined as follows: T is the element temperature, T_c is the heat sink temperature, G is the differential thermal conductance of the heat link defined as the derivative of the conducted power with respect to element temperature T, and k is the function describing the temperature dependence of the thermal conductivity of the heat link material. In the Johnson noise formula, P is the dc bias power dissipated in the element, R is its resistance (= E/I), where E is the bias voltage and I is the bias current, Z is the differential impedance dE/dI, and A is given by $A = -\frac{d\log R}{d\log T}$. It is assumed here that R is a function of temperature alone. The physical time constant τ is given by C/G, and is distinct from the effective time constant τ_e that governs the pulse response in Eq. 2.

Since the frequency dependence of the terms in NEP^2 are simple, the energy resolution can be computed easily as

$$\Delta U_{rms} = \tau^{1/2} \left(N_2(N_1+N_2)\right)^{1/4} \quad . \tag{10}$$

To proceed further, we need to parametrize electrical and thermal characteristics of the detector. We shall assume that the heat capacity, the resistance of the detector, and the thermal conductivity of the support wires are power laws in temperature: the heat capacity $C = C_o\, t^\gamma$, where C_o

is the heat capacity at the bath temperature T_c, the reduced temperature is $t = T/T_c$, the resistance is $R = R_o\, t^{-A}$, and the heat link conductivity is $k = k_o t^{\beta}$. Note that t is not the time t used in Eqs. 2 and 3.

We now wish to determine N_1 and N_2 in terms of these parameters. We take

$$\frac{dP}{dT} \equiv G = k(T)\left[\int_o^x dx/A(x)\right]^{-1} = G(T_c)t^{\beta} \tag{13}$$

from Eq. 24 of Ref. 7 where A (x) is cross section area of the link. Substituting $P = EI = I^2R(T)$ into the heat balance equation permits the calculation of static current-voltage curves and the dynamic response to an energy impulse, and leads to Eq. 2. Using Eq. 13, and the parametric representation for R(t), extensive algebraic manipulation yields

$$\frac{Z+R}{Z-R} = -GT/PA \tag{14}$$

and

$$P = GT(1-t^{-(\beta+1)})/(\beta+1) \tag{15}$$

so that we can find

$$N_2 = 4k_B\, TP(GT/PA)^2$$

$$= 4k_B T_C^{\,2}\, t^2\, G(\beta+1)/A^2\,(1 - t^{-(\beta+1)}). \tag{16}$$

The value of N_1 is found more directly from the defining integrals as

$$N_1 = \frac{4k_B T_C^{\,2} G t^2 (1-t^{-(3+2\beta)})(\beta+1)}{(3+2\beta)(1-t^{-(\beta+1)})}\,. \tag{17}$$

When these expressions are substituted into Eq. 10, we obtain the final formula

$$\Delta U_{rms} = \left[(k_B T_C^2 C_o) \frac{4(\beta+1)t^{2+\gamma}}{A^2(1-t^{-(\beta+1)})} \left[1 + \frac{(1-t^{-(3+2\beta)})A^2}{3+2\beta} \right]^{1/2} \right]^{1/2} \quad (18)$$

Note the very important fact that the thermal conductance G and the time constants τ and τ_e have disappeared entirely from the equation. This means that there is no sensitivity penalty nor advantage to fast or slow detectors, and heat link parameters may be chosen to satisfy other constraints (e.g. counting rates). Moreover, the resolution is a dimensionless factor multiplying the fundamental thermodynamic fluctuation $(k_B T_C^2 C_o)^{1/2}$. Finally, it is important to note that as A approaches infinity, ΔU_{rms} tends to zero as $1/A^{1/2}$, confirming the statement made above that the measurement uncertainty can be less than the thermodynamic energy fluctuations of Eq. 1.

The detector reduced temperature t is the only variable in Eq. 18 which is not already fixed by the available refrigerator (T_C) or the detector construction (C_o, A, β, γ). The value of t is determined by the DC bias power applied. A simple numerical optimization may be easily performed on the expression, yielding both the desired operating temperature and the ultimate sensitivity given the constraints.

An optimum bias power exists because low values of t correspond to low bias currents and low detector response, reducing the signal below the level of the Johnson noise in the thermometer resistance, while high values of t increase the random thermal fluctuation of the detector energy.

Values of A from 2 to 10 are typical for semiconducting thermometers, although A = -100 to -1000 can be achieved for superconducting transition-edge detectors. Values of β are typically 1 for metals, and 3 for dielectric crystals, while γ will be 1 for normal metals and 3 for pure dielectric crystals and for superconductors well below their transition temperatures.

The results of the optimization for several values of γ and β are given in Fig. 2. The optimal temperature t changes only slightly with A, and $\Delta U_{rms} = \xi(k_B T_C^2 C_o)^{1/2}$ is also a weak function of A for A > 2.

III. Amplifier Noise and Load Resistor

The optimization we have carried out does not include the amplifier noise contribution to total system noise. This can be justified because for proper choice of detector resistance and amplifier JFET, the amplifier noise can be made small compared to the noise of the detector, even for detector temperature as low as 0.1 K.

According to Mather's noise theory,[6] the Johnson noise of a bolometer can be reduced by electro-thermal feedback for $\omega \tau < 1$ by as much as 50%. However, in this frequency range the detector also detects its phonon noise, so that the total voltage noise in the signal band of the detector ($\omega\tau<1$) is found to be greater than the Johnson noise in a resistor of equal resistance operating at the same temperature. We will compare this noise to that of the amplifier for two cases: 1) where the bolometer's

resistance can be chosen to minimize the effects of amplifier noise, and 2) where the bolometer must be $\sim$ 10 MΩ to prevent long electrical time constants due to stray capacitance.

The JFETs typically used as bolometer amplifiers (2N4867A) have voltage noise $e_n(f) \lesssim 5\times10^{-9}$ V/$\sqrt{\text{Hz}}$, while measurements in our laboratory give a current noise $i_n(f) \leq 3\times10^{-17}$ A/$\sqrt{\text{Hz}}$. The value of input resistor for which the ratio of total amplifier noise to resistor Johnson noise is a minimum can be shown to be $R_n = e_n/i_n$. For our typical devices $R_n \sim 1.7\times10^8$ Ω. The Johnson noise is

$$e_J(f) = (4 k_B TR)^{1/2} \quad \text{V}/\sqrt{\text{Hz}}. \tag{19}$$

The corresponding total amplifier noise is

$$e_A(f) = (i_n^2(f) R^2 + e_n^2(f))^{1/2} \quad \text{V}/\sqrt{\text{Hz}}. \tag{20}$$

If we are free to choose $R = R_n$, and if our detector noise temperature is 0.1 K, the amplifier voltage contribution is less than 25% of the detector noise. Added in quadrature, it produces less than a 3% increase in system noise. If we are forced to choose a resistance near 10 MΩ for the device, the amplifier noise voltage is 67% of the detector noise, resulting in a 20% increase in system noise. These are upper limits to the effects of amplifier noise, since in practice the bias power can be adjusted slightly to a point which is optimum in the presence of the additional voltage noise.

Load resistor noise cannot be avoided, but can be made negligible by choosing the resistance much larger than the detector resistance. If the load resistor is 10 times the detector resistance and operates at the detector heat sink temperature, it increases detector noise about 5%. A more complete discussion of the load resistor noise contribution is given in Ref. 7.

IV. Sample Detector Design

We have calculated the characteristics of a complete detector design as an example of the performance which might be obtained in practice. Rather than trying to achieve the ultimate in resolution, we have chosen a design which uses established integrated circuit fabrication and silicon etching techniques at tolerances well within their routine capabilities. All materials used have well-known thermal properties, with measured values near the proposed operating temperature available from the literature. The detector construction is shown in Fig. 1, and the heat capacities of each component are given in Table 1.

The thickness of the absorber is chosen to have reasonable stopping efficiency for x-rays up to 9 keV, and the 0.5 mm x 0.5 mm size is suitable for use with many focussing instruments. With all addenda, the net heat capacity is then 5.8×10^{-15} J/K at 0.1 K, resulting in thermodynamic energy fluctuations of 0.18 eV rms. For an effective γ equal to 2.4 and $\beta = 3$, the results of the previous section give an energy resolution of 1.1 eV FWHM, where we have assumed a conservative value of 4.0 for A (the logarithmic temperature sensitivity of the thermistor). The time constant τ is about 300 μsec, giving an NEP of the order of 5×10^{-18} W/Hz$^{1/2}$.

V. Detector Efficiency Variations and Resolving Power Limits

At least five processes may modulate the responsivity of the detector. Random variations of these factors can limit the resolving power ($U/\Delta U$) of the detector. These factors are: 1. The x-ray energy may be carried by a photoelectron which escapes from the detector before depositing its full energy. 2. Excited electrons and excitons may emit photons which escape from the detector. 3. Energy may be held in metastable states that are long-lived with respect to the readout process. 4. The deposited energy may not be uniformly converted into a thermal spectrum of phonons before the phonons leak out through the support legs. 5. The detector may have a nonuniform response across its face, related to the proportion of the deposited energy which reaches the thermometer before going down the support legs.

Photoelectron Escape

A few photoelectrons produced near the detector surface will escape through that surface without depositing their full energy. The fraction which escapes is of the order of ℓ_e/ℓ_x, where ℓ_e is the electron range and ℓ_x is the x-ray mean free path. This is maximum just above an absorption edge, and for Si at 1.6 KeV is $\sim$ 6%. In principle this could be overcome or improved by coating the detector with a low Z material, having a very low ℓ_e/ℓ_x. However, choices are limited by heat capacities at low temperatures.

Radiative Losses

The interaction of an x-ray with a Si crystal results in approximately 30% of the energy being converted to free holes and electrons, with the rest of the energy being converted directly to phonons. Many of the free holes and electrons form excitons, bound hole-electron systems, which decay by emitting phonons, photons, or Auger electrons. Most excitons decay by channels which give rise to rapid thermalization, but some small fraction may decay radiatively. Si is quite transparent to those photons and they can escape from the detector. If on the average N of these photons escape, their statistics would limit the energy resolution to $\sim (N)^{1/2}$ eV. Fortunately, most excitons decay rapidly by nonradiative processes. Hole-electron recombination on a neutral donor is very fast and in the case of As in Si decays by an Auger process within 80 ns.[8,9] The radiative lifetime for such a recombination is 750 μs, so radiative decay is very unlikely. However, there are some traps for which the Auger process is forbidden, and thus have a reasonably high radiative efficiency. Some solutions to this potential radiative loss problem are to 1) produce material without radiatively efficient traps, 2) put a sufficient number of neutral donors in the crystal to dominate undesirable traps, or 3) metallize the external surface of the detector with aluminum to prevent loss of photons created by radiative decays. Detailed studies of radiative loss and heat capacity as a function of donor concentration could be necessary if radiative loss is important.

Metastable States

Another potential difficulty is that the thermalization of part of the deposited energy may be delayed beyond the readout time, resulting in lost energy, with the statistical fluctuations which this implies. Long hole-electron recombination times or long exciton decay time would result in the delayed thermalization. However, if a sufficient donor concentration can be tolerated, the exciton recombination rate will be fast.[8]

If undesirable trapping centers cannot be eliminated or swamped by short-lived sites, it should still be possible to reduce their effects by "flashing" the device to fill the undesirable traps and prevent loss of signal.

Nonthermal Phonon Spectrum

A fourth potential problem is the fact that the spectrum of phonons in the detector following the incidence of an x-ray may be highly nonthermal. Measurements of bulk CaF_2 at 4 K following the impact of an energetic electron shows that after 100 ns the spectrum has relaxed to that of a gray body at about 30 K. The spectrum changes little more for times as long as 2 μs.[10] Therefore, it is possible that the spectrum in our detectors might also remain nonthermal for a time scale on the order of 100 μs. If the spectrum has relaxed to as low a temperature as 30 K, however, it seems that the relative statistical fluctuations in all subsequent processes would be limited to the square root of the number of phonons existing at this temperature as a worst case. This would result in about a 4 eV FWHM uncertainty in the response to a 6 keV x-ray. Given the large surface to volume ratios for these thin detectors, the spectrum may thermalize more

rapidly. The importance of this problem depends on how the thermometers work: if the resistance change of the thermometer is simply a function of the elastic strain energy density, then it should make no difference what spectrum the phonons have. If single quantum processes are important (phonon-assisted hopping), the spectrum may be relevant.

Thermal Uniformity

Since the phonon mean free path in the pure silicon absorber at 0.1 K is much larger than the dimensions of the device, the thermal conductivity is limited by the smallest dimension. The thermal diffusion time τ_d across the 0.5 mm square absorber is then $\sim$ 2 μs if we assume completely diffuse reflection of phonons at the silicon surfaces. However, these etched surfaces are very smooth on the scale of a mean phonon wavelength. Perfect specular reflection of phonons would shorten the diffusion time to $\sim$ 0.2 μs. To ensure uniform response across the surface of the detector, the thermal time constant ($\tau \equiv C/G$) must be long in comparison with this equilibration time for the absorber which is on the order of the phonon crossing time. The fractional variation of response across the face of the detector could be τ_d/τ if no special techniques are employed. The surfaces of the support legs could be roughened by an anisotropic etch, if necessary, to ensure diffuse reflection and decrease their conductance. The resulting thermal time constant using the roughened legs is $\sim$ 300 μs. If specular reflection reduces the absorber relaxation time, the support legs could be shortened to increase G somewhat and allow higher counting rates. It will be difficult to provide sufficiently fast amplifier input risetimes for detector time constants much shorter than 100 μs, however, since the detector resistance must be 10^7 Ω or greater to provide an

adequate match to the JFET noise impedance, and stray capacitances amount to several pF.

We have one concept for measuring the energy deposited in the detector, with a constant responsivity regardless of the location of the x-ray. The detector in Fig. 1 would be modified to have four matched thermometers located at the corners of the silicon absorber and connected in series. The four thermometer regions detect the heat as it flows out of the absorber, and their outputs are added, since they are connected in series. If all the thermometer regions are identical and all the support legs are identical, then the area under the detected pulse shape is strictly proportional to the deposited energy. While pulse shapes may vary slightly as a function of the x-ray position, the total energy should be correctly determined.

We have proposed several effects which may contribute to the uncertainty of the energy of an incident photon. These sources of "thermalization noise" are discussed, and possible remedies are suggested. Preliminary experimental results on a detector have not shown any large nonthermal effects of this type.[11] The tests did not have enough sensitivity to be definitive for a potential 1 eV FWHM detector, however, so a final answer must await further experiments. Given the low efficiency of radiative exciton decays, and the evidence for prompt recombination, we believe these two problems will not be serious. The effects of a possible nonthermal phonon spectrum are not known, but experimental results are in good quantitative agreement with the response expected for a fully thermalized phonon spectrum.[11]

VI. Summary

We propose a thermal detector as an efficient high resolution x-ray spectrometer. A theory for the resolution of the detector as a function of its physical parameters has been presented. For a given detector design and cryostat temperature, the detector temperature, controlled by its bias power, is the only free parameter. We derive the maximum resolution of a given detector for the optimal value of this parameter. The model assumes that the Johnson noise dominates all other noise sources in the thermistor, which has been shown to be the case in other work. This and thermodynamic fluctuations in the detector temperature represent the major noise sources in detectors of this kind. We show that amplifier noise is not a serious problem.

A design is given for a detector capable of operating with good efficiency up to energies of 9 KeV. Assuming noiseless thermalization of the x-ray energy, a resolution of 1.1 eV FWHM is achievable with this device at a heat sink temperature of 0.1 K.

We discuss the possibility of excess noise caused by statistical fluctuations in any energy which is lost or whose thermalization is delayed. Several mechanisms are suggested which may give rise to energy loss, and possible solutions are presented. Further work is required to understand the magnitude of these possible effects and the effectiveness of our proposed solutions.

We believe these detectors show great promise as high resolution x-ray spectrometers and as sensitive microcalorimeters for other measurements. Further laboratory work is necessary to define the limits to their utility.

VII. Acknowledgments

We thank R. Mushotzky for helpful discussions, and D. Arbogast, R. Petre, and G. Lamb for their efforts in preparing and executing experiments to test the theory reported here.

This work is an extension of research on thermal detectors carried out under the NASA Infrared Detector Development program.

TABLE I

THERMAL PROPERTIES OF THE DESIGN ILLUSTRATED IN FIG. 1

Component	Volume (cm^3)	Heat Capacity at 0.1 K ($J\ K^{-1}$)
Intrinsic silicon	6.7×10^{-6}	4.5×10^{-15} (a)
Thermistor implant	1.0×10^{-9}	8.6×10^{-16} (b)
Implanted arsenic contacts	2.0×10^{-10}	1.7×10^{-16} (c)
Aluminum metalization	3.4×10^{-9}	2.4×10^{-16} (d,e,f)

Total heat capacity at 0.1 K: $C_o = 5.8\times10^{-15}$ J K^{-1}

Thermal conductivity of silicon support legs at 0.1 K: $G_o = 1.8\times10^{-11}$ watts K^{-1}

Thermal time constant: $\tau_{th} = CG^{-1} = 320$ μs

$(k_B T_o^2 C_o)^{1/2} = 2.8\times10^{-20}$ J = 0.18 eV

From optimization, as in Fig. 2, $\xi = 2.56$ (For $\gamma_{eff} = 2.4$, $\beta = 3$, $A = 4$)

Energy resolution: $\Delta E_{rms} = 0.45$ eV, or 1.1 eV FWHM

[a] Debye specific heat with $T_D = 630$ K was used. By analogy, for high purity Ge, the 0.1 K specific heat is equal to the Debye value for short time $\tau \sim$ 100 μs, but is about double this value for long times $\tau \geq 10$ ms (M.T. Loponen, R. C. Dynes, V. Narayanamurti, and J. P. Garno, Phys. Rev. B, 25, No. 2, 1161 (1982).

[b] J. R. Marko and J. P. Harrison, Phys. Rev. B, 10, 2448 (1974).

[c] Specific heat from free-electron Fermi gas model.

[d] N. E. Phillips, Phys. Rev., 114, 676 (1959).

[e] N. E. Phillips, Ann. Acad. Sci. Fennicae, A VI, #210 (1961).

[f] 0.5% of aluminum was assumed to be in normal state due to unavoidable trapped flux.

Figure Captions

Figure 1. Concept for 1.1 eV FWHM spectrometer. Heat capacities of component materials are listed in Table 1. The design of the device is similar to devices described in Ref. 1, which gives a detailed discussion of the fabrication procedure.

Figure 2. Optimal detector performance and operating temperature as a function of $A = -d \log R / d \log T$. $t = T/T_o$ is the fractional temperature rise of the detector at the optimal operating point. $C = C_o t^{\gamma}$, $G = G_o t^{\beta}$. $\Delta U_{rms} = \xi (k_B T_o^2 C_o)^{1/2}$ where ΔU_{rms} is the rms uncertainty in the measurement of photon energy. Note ξ is almost independent of β and γ. For $A < 2$, $\xi \propto A^{-1}$, for $A > 2$, $\xi \propto A^{-1/2}$. Note that for $\gamma = 1$, there is less heat capacity penalty for operating at higher t, so the optimal value of t is higher than for $\gamma = 3$.

References

1. P. M. Downey, Ph.D. Thesis, MIT (1980).
2. A. E. Lange, E. Kreysa, S. E. McBride, P. L. Richards, and E. E. Haller, Int. J. Infrared Millimeter Waves 4, 689 (1983).
3. P. M. Downey, A. D. Jeffries, S. S. Meyer, R. Weiss, F. J. Bachner, J. P. Donnelly, W. T. Lindley, R. W. Mountain, and D. J. Silversmith, Appl. Opt. 23, 910 (1984).
4. F. J. Low, J. Opt. Soc. Am. 51, 1300 (1961).
5. R. C. Jones, J. Opt. Soc. Am. 43, 1 (1953).
6. J. C. Mather, Appl. Opt. 21, 1125 (1982).
7. J. C. Mather, Appl. Opt. 23, 584 (1984).
8. D. F. Nelson, J. D. Cuthbert, P. J. Dean, and D. G. Thomas, Phys. Rev. Lett. 17, No. 25, 1262 (1966).
9. J. D. Cuthbert, J.A.P. 42, 747 (1971).
10. R. Baumgartner, M. Engelhardt, and K. F. Renk, Phys. Lett. 94A, 55 (1983).
11. D. McCammon, H. Moseley, J. C. Mather, R. Mushotzky, J. Appl. Phys. (companion paper R-5496).

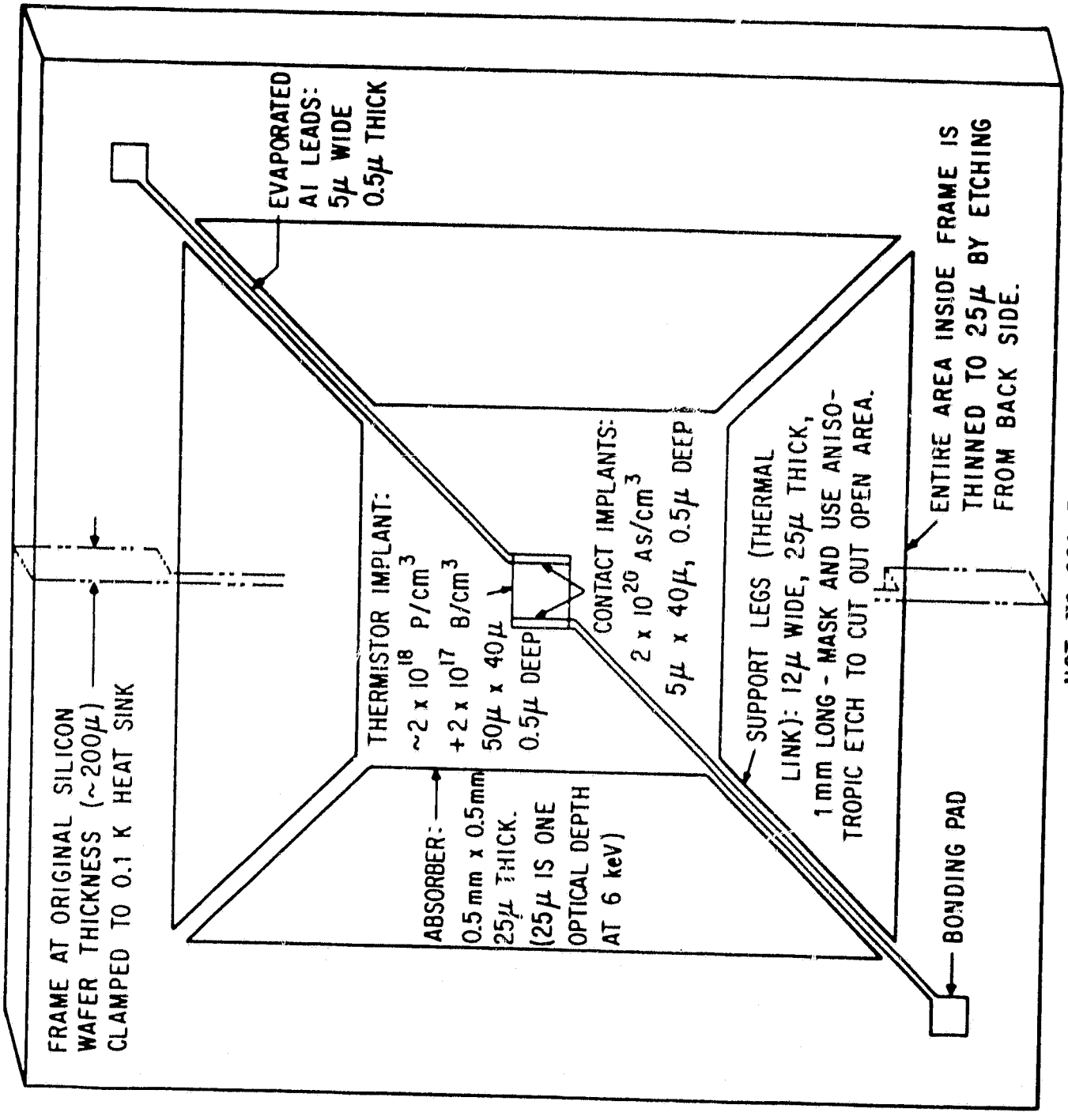

Figure 1

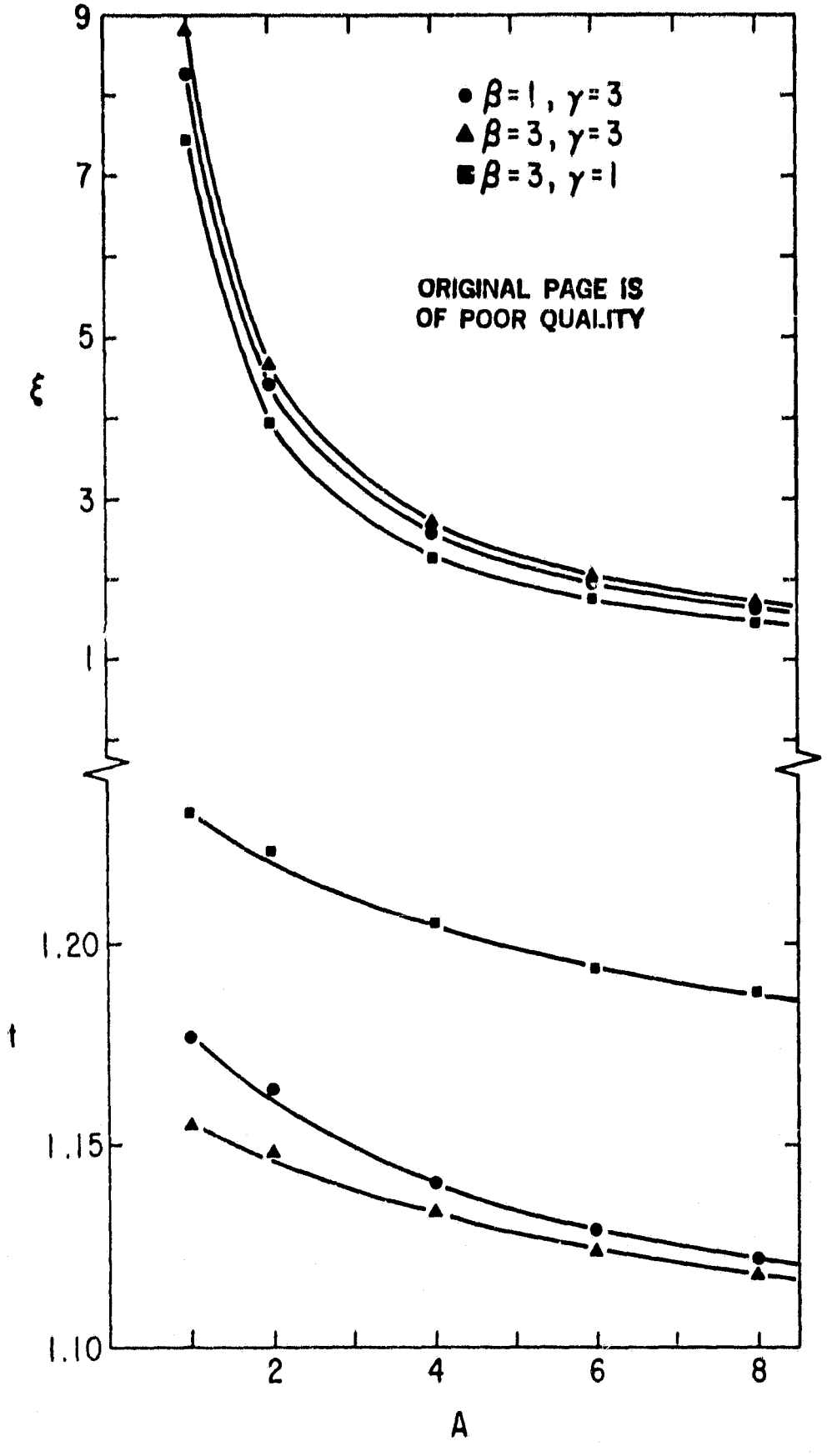
9
7
5
3
1
ξ
● β=1, γ=3
▲ β=3, γ=3
■ β=3, γ=1
ORIGINAL PAGE IS
OF POOR QUALITY
1.20
1.15
1.10
t
2
4
6
8
A

Figure 2